Journal of Hip Preservation Surgery, 2024, **11**, 59–66
DOI: https://doi.org/10.1093/jhps/hnad042
Advance access publication date: 29 November 2023
Research article

The McMaster osteotomy—a novel surgical treatment to chronic slipped capital femoral epiphysis: description of surgical technique and case study

Zhi Li[1], Reva Y. Qiu[1], Abdulaziz Khurshed[1], Dana Alomran[2], Dale S. Williams[3], Olufemi R. Ayeni[2] and Waleed Kishta[2*]

[1]Faculty of Medicine, McMaster University, Hamilton, Ontario L8N 3Z5, Canada, [2]Department of Orthopedic Surgery, McMaster University Medical Center, Hamilton, Ontario L8N 3Z5, Canada and [3]Department of Orthopedic Surgery, Hamilton Health Sciences, Hamilton, Ontario L8L 2X2, Canada

*Correspondence to: Waleed Kishta. E-mail: waleed.kishta@medportal.ca

ABSTRACT

Slipped capital femoral epiphysis (SCFE) is a common adolescent hip disorder that can lead to complex proximal femur deformities and devastating consequences such as avascular necrosis, femoroacetabular impingement syndrome and early-onset osteoarthritis. Existing surgical techniques are often insufficient to fully address the constellation of multiplanar deformities in patients with severe SCFE. Therefore, the McMaster Osteotomy, a novel intertrochanteric proximal femur osteotomy, was developed to improve anatomic correction and hip mechanics in patients with chronic SCFE. The McMaster Osteotomy was implemented in two patients (A: 16-year-old male, B: 17-year-old female) with proximal femur deformities due to chronic SCFE. Surgical planning was facilitated with a 3D-printed pelvic model generated from a CT scan of a patient with the SCFE deformity. Patient B also underwent concurrent arthroscopic osteochondroplasty and labral repair. Pre- and post-operative function and radiographic measurements were recorded. Post-operatively, patient A's neck-shaft angle improved from 125° to 136°, Southwick angle from 52° to 33°, neck length from 66 mm to 80 mm and hip internal rotation from 5° to 25°. Patient B's post-operative neck-shaft angle improved from 122° to 136°, Southwick angle from 25° to 15°, neck length from 76 mm to 84 mm, hip internal rotation from 5° to 20° and alpha angle from 87.6° to 44.3°. Both patients are pain-free and have obtained full union of their osteotomies. The McMaster Osteotomy is a versatile technique that can produce a more anatomic reconstruction of hip anatomy and restoration of abductor mechanics. As an extracapsular technique, the risk of femoral head avascular necrosis is minimized.

INTRODUCTION

Slipped capital femoral epiphysis (SCFE) is a common adolescent hip pathology, affecting 10.8/100 000 adolescents in the United States [1]. While the pathogenesis of SCFE remains to be fully elucidated, high body mass index (BMI) during the prepubertal growth spurt is a noted risk factor [2]. Additionally, SCFE can be associated with endocrine disorders such as hypothyroidism and renal osteodystrophy [2]. The incidence of SCFE is proposed to increase with the obesity epidemic affecting the adolescent population [3, 4].

With SCFE, the proximal femoral physis separates through the hypertrophic zone secondary to excessive mechanical stress, leading to displacement of the metaphysis relative to the epiphysis. This results in complex three-dimensional (3D) deformities and altered hip biomechanics [5–7]. The deformity in SCFE commonly consists of varying degrees of coxa vara, retroversion and extension [8]. Additionally, the displaced metaphysis becomes an osseous protrusion, mechanically abutting the chondrolabral complex which causes early acetabular rim and cartilage damage, leading to secondary femoroacetabular impingement syndrome (FAIS) and early-onset arthrosis [9–12].

In moderate to severe SCFE deformities, proximal femoral osteotomy may be required to restore hip anatomy and improve biomechanics. The modified Dunn's procedure is intended to achieve anatomical restoration of the proximal femur through surgical hip dislocation. However, this technique has a high rate of reported complications, including avascular necrosis (AVN) of the femoral head, non-union and hip dislocation [13, 14]. In contrast, extracapsular osteotomies such as the Southwick and Imhauser techniques have been reported to have lower risk of AVN [15, 16]. However, these techniques are often inadequate to fully address the constellation of deformities in patients with severe slip including femoral neck shortening secondary to premature physeal closure, greater trochanter (GT) overgrowth and altered abductor mechanics [6, 7, 15, 17, 18].

Submitted 25 July 2023; Revised 17 September 2023; revised version accepted 31 October 2023

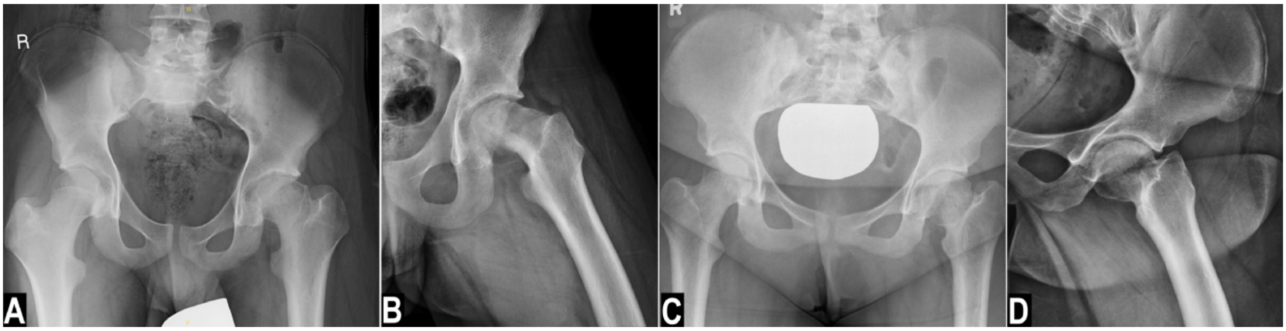

Fig. 1. Pre-operative pelvic and hip radiographs of Patient A and B. (A) Anteroposterior radiograph of the pelvis showing chronic slipped capital femoral epiphysis of the left hip of Patient A. (B) Frog-leg lateral radiograph of the left hip of Patient A. (C) Anteroposterior radiograph of the pelvis showing chronic slipped capital femoral epiphysis of the left hip of Patient B. (D) Frog-leg lateral radiograph of the left hip of Patient B.

The Morscher osteotomy is a true neck-lengthening osteotomy used to treat hip deformities secondary to Legg–Calve–Perthes disease (LCPD) or developmental dysplasia of the hip (DDH) [19, 20]. This technique increases femoral offset and distalizes the overriding GT, thus improving abductor mechanics and reducing extracapsular impingement [21].

The senior surgeons at our institution proposed that by combining the principles of the Imhauser and Morscher osteotomies, a better anatomic reconstruction of the SCFE deformity could be achieved. The purpose of this paper is to describe the surgical techniques of the novel McMaster Osteotomy, and to present its application in the treatment of two adolescent patients with chronic SCFE deformities.

MATERIALS AND METHODS

This study was undertaken at McMaster Children's Hospital. Two patients (Patient A, 16-year-old male, and Patient B, 17-year-old female), with complex proximal femur deformities secondary to chronic SCFE, were included. Informed consent was obtained from both patients.

Case descriptions

Patient A

Patient A started experiencing left knee and hip pain at age 12 and sought an orthopaedic referral in the community at the age of 16. He was diagnosed with chronic SCFE of the left hip and was managed conservatively with regular monitoring. Unfortunately, his pain worsened, and his mobility became limited, prompting referral to our care for a second opinion. He is otherwise healthy.

The patient examination revealed an antalgic gait, positive Trendelenburg test and positive Drehmann sign. He had limited painful hip internal rotation of $<5^\circ$ measured in the supine position with 90° of hip flexion, and positive anterior and posterior impingement tests. He had a true leg-length discrepancy (LLD) of 3 cm of shortening of the affected leg when measured from anterior superior iliac spine (ASIS) to the medial malleolus.

Radiographs showed a closed and healed proximal femur physis with deformities consisting of coxa vara, coxa breva, epiphyseal retroversion, femoral extension and a cam lesion (Fig. 1A and B). The senior authors opted to proceed with a preoperative MRI to rule out any labral or intra-articular hip pathology. MRI revealed early labral degeneration without any obvious labral tear or significant osteoarthritic changes.

Given the clinical and imaging findings, the patient elected to undergo surgical treatment with the McMaster Osteotomy.

Patient B

Patient B was a 17-year-old female at the time of surgery. She had a long-standing history of left lower leg pain with an antalgic gait. She was referred to our institution at age 13 and was eventually diagnosed with a chronic SCFE of the left hip. She is otherwise healthy.

On examination, she walked with an antalgic gait and had a positive Trendelenburg test. She had limited painful hip internal rotation of $<5^\circ$ measured in the supine position with hip in 90° of hip flexion, and positive anterior and posterior impingement tests. She had a clinical true LLD of 3 cm of shortening affecting the ipsilateral leg.

Radiographs showed a closed and healed proximal femur physis with deformities consisting of coxa vara, coxa breva, epiphyseal retroversion, femoral extension and a cam lesion (Fig. 1C and D). MRI showed a large posterolateral labral tear and bony overhang at the superior acetabular rim with localized early osteoarthritic changes.

Given the SCFE deformity and labral pathology, the patient consented to undergo combined arthroscopic hip surgery and McMaster Osteotomy.

Preoperative planning

A 3D-printed model of hemipelvis was generated using a CT scan of a patient with chronic SCFE deformity (Fig. 2). CT scan was obtained from the Hospital Medical Imaging Department server as an anonymized digital imaging and communications in medicine (DICOM) file. The DICOM file was imported into the 3D Slicer software [The Slicer community, Boston, MA, USA]. Segmentation was completed with an automated thresholding protocol within the software to isolate the skeletal element of the hemipelvis and proximal femur. A printable Standard Tessellation Language (STL) file was exported from 3D Slicer and 3D printing was carried out using the Ultimaker Cura program and the Ultimaker 3 Extended 3D printer [Ultimaker B.V.,

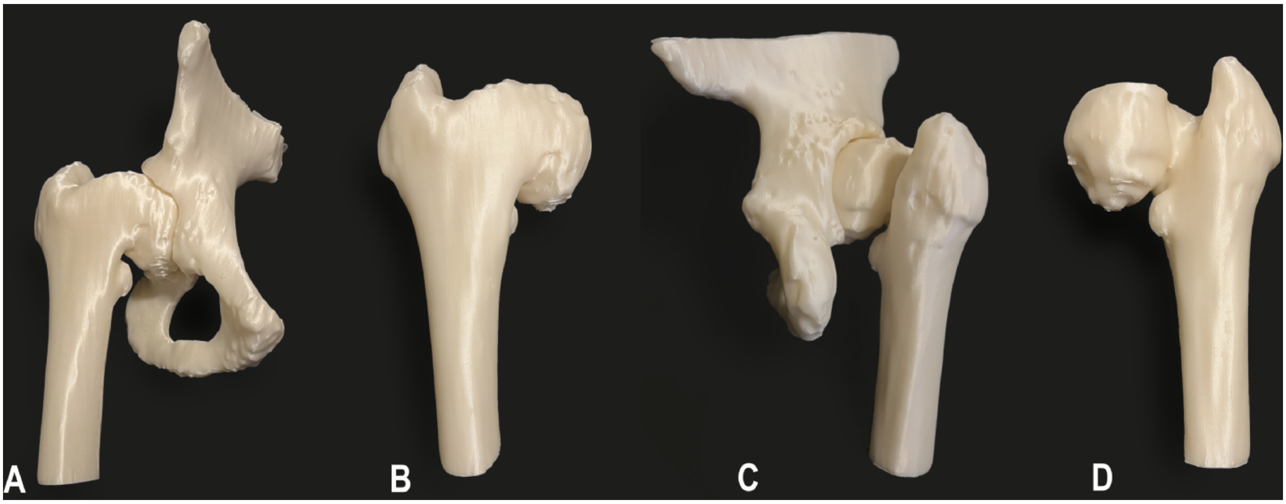

Fig. 2. Three-dimensionally printed models obtained from a patient with chronic slipped capital femoral epiphysis deformity of the hip joint. **(A)** Anterior view of hip and pelvis model showing the external rotation, varus and anterior displacement of the proximal femur metaphysis relative to the epiphysis. **(B)** Anterior view of proximal femur model without the acetabulum and pelvis for better visualization of the proximal femur deformity. **(C)** Posterior view of hip and pelvis model demonstrating the displaced relationship between the proximal femur metaphysis and epiphysis. **(D)** Posterior view of proximal femur without the acetabulum and hemipelvis for better visualization of the proximal femur deformity.

Utrecht, Netherlands]. The 3D model was printed with the factory standard printing protocol using Ultimaker PLA (polylactic acid) filament.

To confirm the degree of achievable correction with our described surgical technique, the 3D model was used by the senior surgeons to plan the osteotomy cuts and deformity corrections illustrated in Fig. 3.

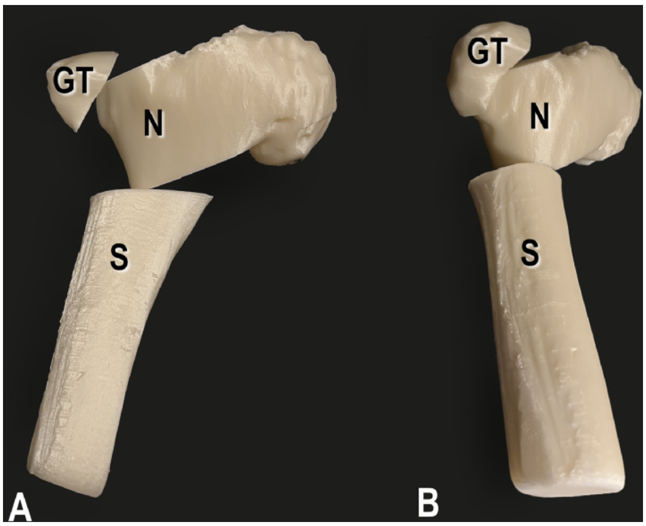

Fig. 3. Three-dimensionally printed models of planned osteotomy cuts and deformity correction. **(A)** Anterior view of the model showing the proposed osteotomy cuts and the deformity correction. Osteotomy cuts parallel to the superior and inferior border of the femoral neck dividing the proximal femur into the greater trochanter (GT), the neck (N) and the shaft (S) segments. Deformity correction in the coronal plane consisted of valgus correction of the femoral neck-shaft angle, internal rotation and lateralization of the femoral shaft, and distalisation of the greater trochanter. **(B)** Lateral view of the osteotomized model showing corrections in the sagittal plane which consisted of internal rotation of the femoral shaft.

Simultaneous hip arthroscopy, labral repair and osteochondroplasty—patient B

Patient B first underwent ipsilateral hip arthroscopy to address the labral tear and FAIS. Patient A did not require concurrent arthroscopic intervention based on MRI findings.

Surgical procedure and intra-operative findings

Patient B was positioned supine on a radiolucent table with the operative extremity under traction. A modified anterolateral portal and mid-anterior portal were utilized for diagnostic arthroscopy. Prominent bony ridges of the acetabulum were noted in the 12–3 o'clock position. Localized partial-thickness cartilage detachment was seen in the superolateral weightbearing rim with patchy areas of exposed subchondral bone, overall articular surface of acetabulum and femoral head were preserved. The small areas of cartilage degeneration were readily mended with arthroscopic resection of the overhanging bony ridges and debridement of the acetabular rim.

The labrum was found to be partially detached from the 9 to 3 o'clock position with intrasubstance fibrillation. For labral repair, four 1.4 mm suture anchors (Nanotack, Stryker, Kalamazoo, MI, USA) were inserted into the 11, 1, 2, and 3 o'clock position to stabilize the labrum.

A distal anterolateral portal was established and a T-capsulotomy was performed. The femoral head had a mushroom cap-like appearance with bony prominence in the anterior head and neck junction.

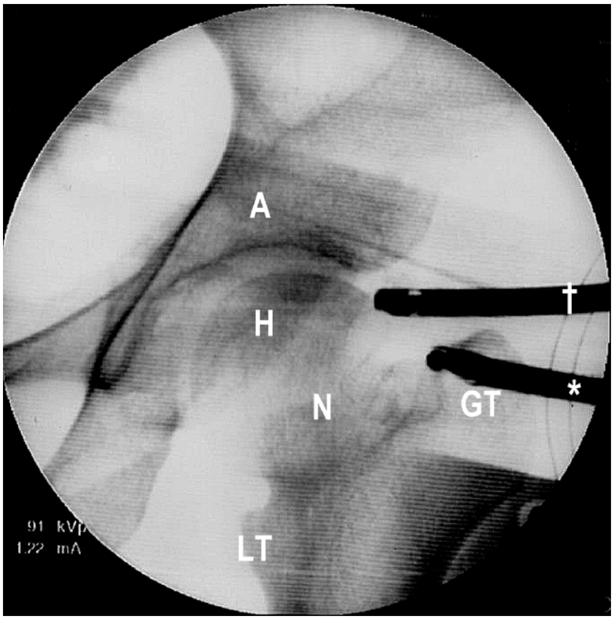

Fig. 4. Intraoperative fluoroscopic image of Patient B showing arthroscopic osteochondroplasty and removal of the bony protrusion at the anterosuperior metaphyseal–epiphysial junction prior to McMaster Osteotomy. †90° arthroscopic camera, *Arthroscopic burr; A, acetabulum; H, femoral head; N, femoral neck; GT, greater trochanter; LT, lesser trochanter.

Osteochondroplasty was performed with intraoperative fluoroscopy to decompress the head and neck junction and partially restore the offset and concavity (Fig. 4). Once satisfied with the decompression, the T-capsulotomy was re-approximated and scope portals were closed. Patient B was then repositioned supine onto a radiolucent flat-top table for the McMaster osteotomy.

McMaster osteotomy

Positioning and preparation

The patients were positioned supine on a radiolucent operating table. The operative lower extremity was sterilely prepped and freely draped to allow intra-operative mobilization. Bony landmarks such as the ASIS, femoral condyles, tibial tuberosity, and the medial and lateral malleoli were accessible during the operation for assessment of alignment and rotation of the operative leg.

Surgical exposure

The direct lateral approach of the hip was utilized with a standard incision starting 3 cm above the GT and extending 10 cm distally. Dissection was carried through subcutaneous tissue down to the iliotibial (IT) band and tensor fascia latae (TFL). The IT band was divided in line with the incision to expose the vastus lateralis and hip abductors. The attachment of the vastus lateralis was divided and reflected anteriorly off the GT. For adequate exposure, the lateral proximal femur was exposed just distal to the lesser trochanter (LT) inferiorly.

Osteotomy

A K-Wire was placed down the centre of the femoral neck under fluoroscopic guidance. Three parallel K-wires were then inserted, two wires marking out the superior and inferior borders of the femoral neck, and the third wire through the centre of the GT (Fig. 5A). Using the oscillating saw, the lateral cortex of the intertrochanteric and subtrochanteric areas were lightly scored and marked with marking pen to guide de-rotation and alignment of the osteotomy.

The GT osteotomy was performed first. Using the oscillating saw, the superior K-wires were used to guide mobilization of the body of the GT with gluteal muscle attachment. A second osteotomy was completed at the base of the GT parallel to the superior border of the neck, obtaining a wafer of bone approximately 5–10 mm thick to be used as a bone graft for the elongation of the femoral neck. Given the proximity to the piriformis fossa, special care was taken to protect the branches of the medial femoral circumflex artery, the main blood supply to the femoral head when performing these osteotomy cuts. Specifically, the GT osteotomy was performed under fluoroscopic guidance, and the saw was used for the lateral 90% of the cut, and then the GT osteotomy was carefully completed with an osteotome.

Lastly, a third cut was made at the level of the inferior border of the femoral neck using the inferior K-wire as a guide. At the completion of the osteotomy cuts, the proximal femur was divided into four segments: GT, graft, neck and distal shaft.

Deformity correction

The LCP Pediatric Plate System (DePuy Synthes, Raynham, MA, USA) was used for fixation following deformity correction.

Based on preoperative planning, the 5 mm 130° plate was used for both cases to achieve the neck-shaft angle correction to match the contralateral hip. Under fluoroscopic guidance, a guide wire for the locking plate was inserted down the centre of the neck of the femur using the 130° guide. To achieve the desired flexion correction of the proximal femur, the guide was rotated anteriorly, and two additional guide wires placed through the guide to determine the final orientation of the plate. The bone graft, along with the plate, was then fixed proximally onto the lateral cortex of the neck with three 5 mm locking screws, thus achieving the desired neck lengthening (Fig. 5B).

Next, the distal femur shaft was reduced to the plate and the proximal femur segment to correct the external rotation, coxa vara and extension deformities. De-rotation of the femoral shaft was done based on preoperative and radiographic assessment. The degree of external rotation correction was assessed using anatomical landmarks and the marking on the lateral cortex. In addition, the varus and extension deformities were corrected as the distal femoral shaft was reduced onto the plate (Fig. 5C). The goal at the completion of the deformity correction was to achieve 10–15° of hip anteversion, over 90° of hip flexion and 30–40° of symmetrical internal and external hip rotation measured with the hip in extension and 90° of flexion. This is to help facilitate activities such as sitting, navigating stairs and tying shoes.

Trochanteric transfer

The GT transfer was done with the hip in 20–30° of abduction. Under fluoroscopic guidance, the GT segment was advanced

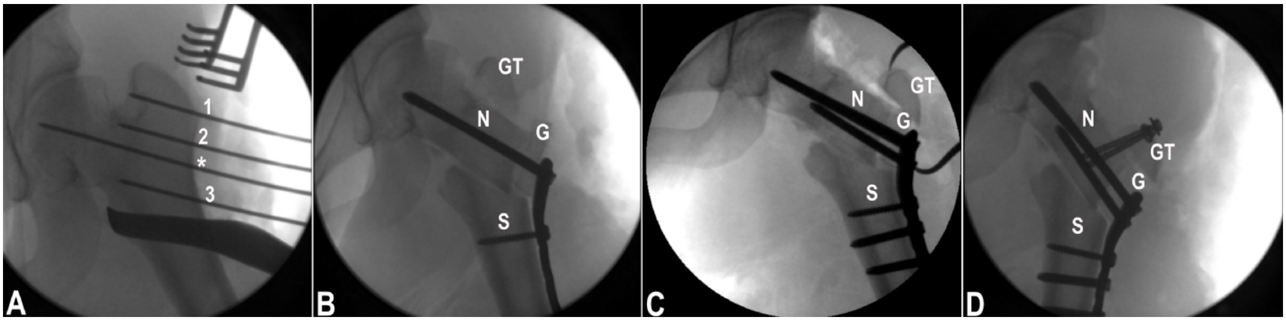

Fig. 5. Intra-operative fluoroscopic images patient B undergoing left hip McMaster osteotomy. **(A)** K-wires making out the centre of the femoral neck (*), and planned locations for osteotomy at the greater trochanter (1), superior border of the femoral neck (2), and inferior border of the femoral neck (3). **(B)** Post-osteotomy, the proximal femur divided into the greater trochanter (GT), graft (G), neck (N) and shaft (S) segments. Osteotomy fixation with proximal femur locking plate showing the incorporation of the graft to the lateral cortex of the neck segment for femoral neck lengthening. The distal shaft segment is then reduced to the neck with the plate in flexion, internal rotation and abduction to restore the neck-shaft angle and proper alignment of the proximal femur. **(C)** The greater trochanter segment is distalized to the appropriate position with a large pointed reduction clamp prior to fixation. **(D)** The greater trochanter is fixated in the distalized position with two 4.5 mm cannulated screws with washers.

laterally and distally until the tip of the GT was located at the same level as the centre of the femoral head. The GT segment was fixated using two 4.5 mm cannulated screws with washers (Fig. 5D).

Table I. ***Summary of the post-operative protocol based on clinical and radiographic assessment***

Post-operative protocol
Phase I: Healing and reparative phase (0–2 weeks)
• Strict non-weight bearing protocol on the operative extremity
• Passive hip ROM restricted to under 90 of flexion
• No active hip abduction, internal or external rotation
Phase II: Mobility and neuromuscular retraining (2–4 weeks)
• X-ray at 2 weeks post-operation to reassess fixation and deformity correction
• Strict non-weight bearing protocol on the operative extremity
• Initiate gentle passive and active assisted ROM
Phase III: Muscle balance and strengthening. (6–12 weeks)
• Repeat X-ray at 6 weeks post-operation for fixation stability and osteotomy healing
• Progressive increase in weight bearing allowed starting at 6 weeks post-operation
• No restriction on ROM
Phase IV: Return to pre-operative activity level (>12 weeks)
• Repeat X-ray at 12 weeks and 6 months to assess for fixation stability and osteotomy healing
• Achieving full weight bearing and independent ambulation
• Assess and address any remaining deficits in ROM, strength and mobility
• Initiate progressive resistance training starting after 12 weeks
• Gradual return to sports starting at 6 months
* Progression to the next phase is based on radiographic healing and fixation stability. i.e. no fixation loosening, well maintained deformity correction, and interval bony callus formation and osteotomy healing

ROM—Range of motion.

Post-operative protocol

Both patients followed a strict non-weightbearing protocol on the operative extremity for the first 6 weeks (Table I). During the first 2 weeks (the healing and reparative phase), passive hip range of motion (ROM) was restricted to <90° flexion with no active abduction or internal/external rotation. Gentle passive and active-assisted ROM were allowed at 2 weeks post-surgery, and gradually progressed to ROM was as tolerated without restrictions by 6-week post-operative mark. Given radiographic evidence of bone healing, progressive increase in weightbearing was permitted and advanced to full weightbearing by post-operative week 12. Gentle resistance training was then started and progressed to full activity without restrictions at 6 months post-surgery.

Radiographs were taken at 2 weeks, 6 weeks, 12 weeks, 6 months, 12 months and 18 months post-operation. Radiographic findings of bone healing, neck-shaft angle, and Southwick angle were examined and documented. Hip ROM and general mobility/function were evaluated clinically at each follow-up starting at 6 weeks postoperation.

RESULTS

The operative time for the McMaster Osteotomy was approximately 180 min. An additional 120 min was used for arthroscopic labral repair and osteochondroplasty for Patient B. The estimated blood loss for both of the cases was 400 ml; no blood transfusion was required for either of the patients. The patients tolerated the procedure well without any complications after 18 months of follow-up. Postoperative radiographs showed progressive bony healing without evidence of hardware or fixation failure. The hip biomechanical parameters including the femoral offset, neck length and neck-shaft angle were reconstituted to match the contralateral unaffected hip.

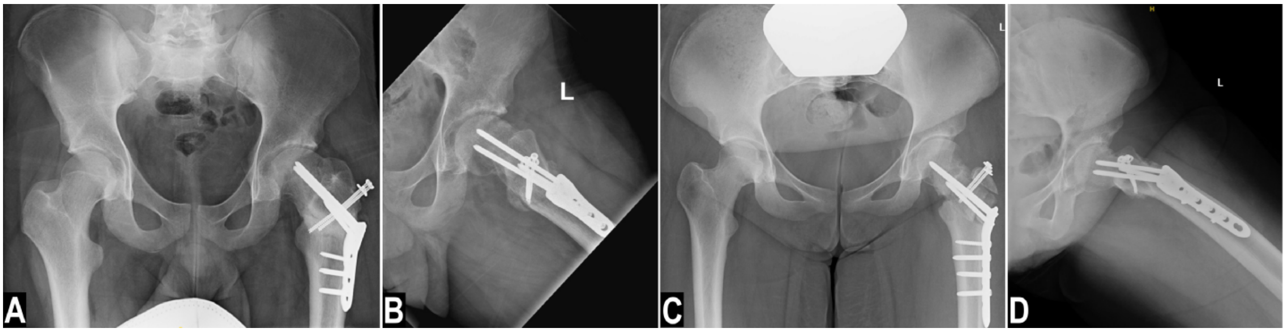

Fig. 6. Post-operative radiographs of Patient A and B following McMaster Osteotomy of the proximal femur. **(A)** Anteroposterior radiograph of pelvis with deformity correction in the left hip of Patient A. **(B)** Frog-leg lateral radiograph of the left hip of Patient A. **(C)** Anteroposterior radiograph of pelvis with deformity correction in the left hip of Patient B. **(D)** Frog-leg lateral radiograph of the left hip of Patient B.

Table II. ***Radiographic parameters of patients' hip of pre- and post-deformity correction***

	Patient A			Patient B		
	Pre-op	Post-op	Contralateral*	Pre-op	Post-op	Contralateral*
Neck-shaft angle	125°	136°	140°	122°	136°	137°
Southwick angle	52°	33°	14°	25°	15°	3°
Neck length	66 mm	80 mm	78 mm	76 mm	84 mm	84 mm
Alpha angle	–	–		87.6°†	44.3°†	–

*Unaffected contralateral side used as control for comparison.
†Only patient B underwent additional concurrent osteochondroplasty for cam deformity correction.

Patient A

Patient A had an uncomplicated recovery course and was discharged on post-operative day (POD) 3. He was ambulating without assistance by 12 weeks post-operation. His internal hip rotation improved from 5° to 25° with pain-free ROM. He continued to have a mild limp secondary to a residual 2.4 cm shortening of the left leg confirmed on post-operative scanogram. The LLD was managed with a shoe lift. At 15 months follow-up, he was carrying out daily activities without concerns.

On radiographic assessment, his neck-shaft angle improved from 125° to 136° and his Southwick angle improved from 52° to 33° (140° and 14° on contralateral side). Neck length improved from 66 to 80 mm (78 mm on contralateral side) (Table II; Fig. 6A and B).

Patient B

Patient B was discharged on POD 5. Her recovery progress was slower compared to Patient A and she began to transition off crutches after her 12 weeks post-operative follow-up. She had an additional visit at 4 months post-operation to assess her progress in mobility. At her 6-month follow-up, she was ambulating independently without discomfort. She had notable improvement in her hip ROM with hip internal rotation improving from 5° to 20°. Overall, her pain, mobility, and function have considerably improved compared to her pre-operative state, and both she and her parents are pleased with her recovery.

On radiographic assessment, her neck-shaft angle improved from 122° to 136° and her Southwick angle was corrected from 25° to 15° (137° and 3° on contralateral side). Neck length improved from 76 to 84 mm (84 mm on contralateral side) (Table II; Fig. 6C and D). Alpha angle improved from 88° to 44° (normal alpha angle value is 47.5°) [22].

DISCUSSION

The surgical management of SCFE and the resulting deformities remains challenging. *In situ* fixation is preferred for acute SCFE to stabilize the slip and prevent further progression [12, 23]. However, due to risk of AVN, it is recommended to minimize reduction during the pinning process. Even with the initial surgical management, considerable deformities often remain and can lead to altered anatomy and biomechanics of the hip [7, 10, 24].

Although numerous treatment options exist to address the complex deformities of chronic SCFE, there is no gold standard of treatment. The modified Dunn's procedure and Imhauser osteotomy are common techniques used today. The modified Dunn's procedure produces a more anatomic reconstruction of the proximal femur when compared to the existing extracapsular osteotomy techniques, but it carries a high rate of serious complications [13, 25]. A recent study found a 37% rate of post-operative complications including AVN (23%), nonunion (9%), and post-operative hip dislocation (5%) [14]. The rate of complications increases in skeletally mature patients with healed deformities and closed physis since a clear cleavage plane for realignment would be lacking [9, 17]. In comparison, the Imhauser Osteotomy has a lower risk of AVN, but the correction is less anatomic. In addition, a closed-wedge osteotomy may further shorten the affected limb. In patients treated with the Imhauser osteotomy, 46% had a moderate-to-severe limp due to a combination of gluteal muscle insufficiency and LLD [26]. Such corrective osteotomies below the femoral head may also worsen the abductor dysfunction due to fixed retroversion of the femoral head [17, 27].

The McMaster osteotomy combines the principles of the Imhauser and Morscher osteotomies aimed to mitigate the shortcomings of existing osteotomy procedures and create a more anatomic correction of chronic SCFE deformities. The McMaster osteotomy is capable of correcting coxa vera, retroversion and extension deformities, while simultaneously restoring neck length and femoral offset in a single procedure. Furthermore, as an extracapsular technique, the risk of iatrogenic AVN of the femoral head is minimized.

Previously, studies have found subjective improvement in hip abductor function when combining the Imhauser Osteotomy with distalization of the GT [17]. Utilizing the principle of the Morscher osteotomy, femoral neck length and offset could be restored and thus, improve the lever arm of the hip abductor/gluteal muscles. Combined with distalisation of the GT, this further improves abductor muscle mechanics. Restoring femoral neck length and distalisation of the GT may also reduce the risk of extracapsular impingement, commonly seen after other traditional corrective osteotomies for SCFE deformities [17]. However, the true impact of McMaster osteotomy on the hip biomechanics would need to be assessed in future prospective studies with rigorous clinical evaluations and biomechanical testing.

Most healed SCFE deformities result in a metaphyseal bump at the anterosuperior aspect of the femoral neck which abuts the acetabulum and leads to a cam-type FAIS. This causes partial versus full thickness labral tears at the chondrolabral junction. Our study showed that hip arthroscopy along with the McMaster osteotomy can be safely performed under the same anesthesia for treatment of concomitant labral tears. Studies suggest that combined open osteochondroplasty and intertrochanteric osteotomy (ITO) via surgical hip dislocation may produce better patient-reported outcomes compared to ITO alone in correcting SCFE deformities and associated FAI [28]. However, surgical hip dislocation requires a larger incision, increases surgical complexity and increases risk of AVN. Our technique did not require surgical hip dislocation and the cam deformity and labral pathologies were effectively managed with hip arthroscopy.

The McMaster osteotomy is a versatile technique that would be especially advantageous in treatment of subset of chronic SCFE patients with severe growth disturbances of the proximal femoral physis and the GT, especially seen with patients where the slip occurred at a younger age. The main contraindications of McMaster osteotomy include skeletal immaturity and generalize advanced hip arthrosis.

LIMITATIONS

This retrospective case study is limited by a small patient sample and having conducted at a tertiary centre with specialized expertise. There are several limitations inherent to this type of study such as publication bias, expertise bias and danger of over-interpretation. The follow-up in this study are short term and functional outcomes of patients could be better assessed with validated instruments such as the Oxford Hip Score or the Hip Dysfunction and Osteoarthritis Outcome Score before and after surgery. Additional biomechanical testing of the hip abductor and flexor function would also be required in the future to fully evaluate the impact of this novel technique on the hip biomechanics. Therefore, the extent of clinical benefit of the McMaster osteotomy in patients with chronic severe SCFE deformity remains to the elucidated with future prospective studies with long-term follow-up.

CONCLUSION

Optimal surgical management of SCFE deformities is a challenging and evolving topic. Our study demonstrated the feasibility of the McMaster Osteotomy in treating the SCFE-associated complex deformities. From our preliminary case series, this technique can yield a more anatomic reconstruction of hip anatomy. Furthermore, as an extracapsular technique, this theoretically reduces the risk of iatrogenic AVN of the femoral head. Future prospective studies with long-term patient follow-up will be needed to evaluate the impact of the McMaster osteotomy on patient's functional outcome.

DATA AVAIILABILITY

The data used to support the findings of this study are available within the article. Raw data that support the findings of this study are available from the corresponding author upon request.

FUNDING

None.

CONFLICT OF INTEREST STATEMENT

Olufemi Ayeni MD PhD is a part of the Speakers Bureau for CONMED Corporation and is a Tier 2 Canada Research Chair in Joint Preservation. Dale Williams MD is a recipient of institutional academic grant from Stryker Corporation.

REFERENCES

1. Lehmann CL, Arons RR, Loder RT *et al.* The epidemiology of slipped capital femoral epiphysis: an update. *J Pediatr Orthop* 2006; **26**: 286–90.
2. Novais EN, Millis MB. Slipped capital femoral epiphysis: prevalence, pathogenesis, and natural history. *Clin Orthop Relat Res* 2012; **470**: 3432–8.
3. Murray AW, Wilson NIL. Changing incidence of slipped capital femoral epiphysis: a relationship with obesity?. *J Bone Joint Surg Br* 2008; **90**: 92–4.
4. Perry DC, Metcalfe D, Lane S *et al.*. Childhood obesity and slipped capital femoral epiphysis. *Pediatrics* 2018; **142**: e20181067.
5. Castañeda P, Ponce C, Villareal G *et al.*. The natural history of osteoarthritis after a slipped capital femoral epiphysis/the pistol grip deformity. *J Pediatr Orthop* 2013; **33**: S76–82.
6. Cherkasskiy L, Caffrey JP, Szewczyk AF *et al.* Patient-specific 3D models aid planning for triplane proximal femoral osteotomy in slipped capital femoral epiphysis. *J Child Orthop* 2017; **11**: 147–53.
7. Rab GT. The geometry of slipped capital femoral epiphysis: implications for movement, impingement, and corrective osteotomy. *J Pediatr Orthop* 1999; **19**: 419–24.
8. Wylie JD, Novais EN. Evolving understanding of and treatment approaches to slipped capital femoral epiphysis. *Curr Rev Musculoskelet Med* 2019; **12**: 213–9.
9. Ziebarth K, Leunig M, Slongo T *et al.* Slipped capital femoral epiphysis: relevant pathophysiological findings with open surgery. *Clin Orthop* 2013; **471**: 2156–62.

10. Hosalkar HS, Pandya NK, Bomar JD *et al*. Hip impingement in slipped capital femoral epiphysis: a changing perspective. *J Child Orthop* 2012; **6**: 161–72.
11. Lee CB, Matheney T, Yen YM. Case reports: acetabular damage after mild slipped capital femoral epiphysis. *Clin Orthop* 2013; **471**: 2163–72.
12. Abraham E, Gonzalez MH, Pratap S *et al.* Clinical implications of anatomical wear characteristics in slipped capital femoral epiphysis and primary osteoarthritis. *J Pediatr Orthop* 2007; **27**: 788–95.
13. Sankar WN, Vanderhave KL, Matheney T *et al.* The modified Dunn procedure for unstable slipped capital femoral epiphysis: a multicenter perspective. *J Bone Joint Surg Am* 2013; **95**: 585–91.
14. Upasani VV, Matheney TH, Spencer SA *et al.* Complications after modified Dunn osteotomy for the treatment of adolescent slipped capital femoral epiphysis. *J Pediatr Orthop* 2014; **34**: 661–7.
15. Schai PA, Exner GU. Corrective Imhäuser intertrochanteric osteotomy. *Oper Orthop Traumatol* 2007; **19**: 368–88.
16. Imhäuser G. Imhauser's osteotomy in the florid gliding process. Observations on the corresponding work of B.G. Weber. *Z Orthop Ihre Grenzgeb* 1966; **102**: 327–9.
17. Baraka MM, Hefny HM, Thakeb MF *et al.* Combined Imhauser osteotomy and osteochondroplasty in slipped capital femoral epiphysis through surgical hip dislocation approach. *J Child Orthop* 2020; **14**: 190–200.
18. Sakr MA, Mohammady EM, Elzahhar MS. Correction of deformity associated with healed slipped capital femoral epiphysis by Imhäuser osteotomy. *Benha J Appl Sci* 2021; **6**: 181–6.
19. Faure PA, Zaltz I, Côté K *et al.* Morscher osteotomy through surgical dislocation approach for true femoral neck lengthening with greater trochanter transposition. *J Bone Joint Surg Am* 2020; **102**: 66–72.
20. Hefti F, Morscher E. The femoral neck lengthening osteotomy. *Orthop Traumatol* 1993; **2**: 144–51.
21. Baraka MM, Hefny HM, Thakeb MF *et al.* Morscher's femoral neck lengthening osteotomy through surgical hip dislocation approach for preservation of perthes and perthes-like deformities. *J Child Orthop* 2022; **16**: 5–18.
22. Pollard TCB, Villar RN, Norton MR *et al.* Femoroacetabular impingement and classification of the cam deformity: the reference interval in normal hips. *Acta Orthop* 2010; **81**: 134–41.
23. Tokmakova KP, Stanton RP, Mason DE. Factors influencing the development of osteonecrosis in patients treated for slipped capital femoral epiphysis. *J Bone Joint Surg Am* 2003; **85**: 798–801.
24. Leunig M, Casillas MM, Hamlet M *et al.* Slipped capital femoral epiphysis: early mechanical damage to the acetabular cartilage by a prominent femoral metaphysis. *Acta Orthop Scand* 2000; **71**: 370–5.
25. Sikora-Klak J, Bomar JD, Paik CN *et al.* Comparison of surgical outcomes between a triplane proximal femoral osteotomy and the modified Dunn procedure for stable, moderate to severe slipped capital femoral epiphysis. *J Pediatr Orthop* 2019; **39**: 339–46.
26. Kartenbender K, Cordier W, Katthagen BD. Long-term follow-up study after corrective Imhäuser osteotomy for severe slipped capital femoral epiphysis. *J Pediatr Orthop* 2000; **20**: 749–56.
27. Anderson LA, Erickson JA, Severson EP *et al.*. Sequelae of perthes disease: treatment with surgical hip dislocation and relative femoral neck lengthening. *J Pediatr Orthop* 2010; **30**: 758–66.
28. Abdelaziz TH, Elbeshry SS, Goda AH *et al.* Intertrochanteric Imhäuser osteotomy combined with osteochondroplasty in treatment of moderate-severe stable slipped capital femoral epiphysis: a case series study. *J Pediatr Orthop* 2020; **29**: 283–91.